Published online 11 July 2011 *Nucleic Acids Research, 2011, Vol. 39, No. 19* ***8445–8456***
doi:10.1093/nar/gkr435

Role for hACF1 in the G2/M damage checkpoint

Sara Sánchez-Molina[1,2], Oliver Mortusewicz[2,3], Béatrice Bieber[1,2], Susanne Auer[4,5], Maren Eckey[1,2], Heinrich Leonhardt[2,3], Anna A. Friedl[4] and Peter B. Becker[1,2,*]

[1]Adolf-Butenandt-Institute, [2]Center for Integrated Protein Science (CIPSM), [3]Department of Biology II, [4]Department of Radiation Oncology and [5]Institute of Cell Biology, Ludwig-Maximilians-University Munich, Germany

Received February 1, 2011; Revised April 29, 2011; Accepted May 12, 2011

ABSTRACT

Active chromatin remodelling is integral to the DNA damage response in eukaryotes, as damage sensors, signalling molecules and repair enzymes gain access to lesions. A variety of nucleosome remodelling complexes is known to promote different stages of DNA repair. The nucleosome sliding factors CHRAC/ACF of *Drosophila* are involved in chromatin organization during development. Involvement of corresponding hACF1-containing mammalian nucleosome sliding factors in replication, transcription and very recently also non-homologous end-joining of DNA breaks have been suggested. We now found that hACF1-containing factors are more generally involved in the DNA damage response. hACF1 depletion increases apoptosis, sensitivity to radiation and compromises the G2/M arrest that is activated in response to UV- and X-rays. In the absence of hACF1, γH2AX and CHK2ph signals are diminished. hACF1 and its ATPase partner SNF2H rapidly accumulate at sites of laser-induced DNA damage. hACF1 is also required for a tight checkpoint that is induced upon replication fork collapse. ACF1-depleted cells that are challenged with aphidicolin enter mitosis despite persistence of lesions and accumulate breaks in metaphase chromosomes. hACF1-containing remodellers emerge as global facilitators of the cellular response to a variety of different types of DNA damage.

INTRODUCTION

The recognition and repair of DNA damage requires that signalling molecules and repair enzymes gain access to the lesions, and hence necessitates extensive chromatin reorganization. At the structural level of chromosomal domains, the predominant mechanisms of regulating the access to the genome involve histone modifications (1–5). At the level of the chromatin fibre nucleosome remodelling enzymes are involved in all processes that assure the integrity of complex genomes: the faithful assembly of the chromatin fibre in the context of replication, the remodelling of chromatin to render lesions accessible to the repair machinery and the regeneration of the integrity of the chromatin fibre once the DNA has been repaired. Nucleosome remodellers modulate the interactions of histones with DNA and are thus involved in nucleosome assembly and disassembly, in the replacement of nucleosomal histones by variant forms and the movement and positioning of nucleosomes on DNA (6). Their local action on single nucleosomes may have profound effects on higher order chromatin structure (7). Clearly, nucleosome remodelling is an integral aspect of the cellular response to DNA modifications induced by chemicals or UV radiation that hinder the replication, or DNA double-strand breaks (DSB) generated by ionizing radiation (6,8–11). Although, the precise role of remodellers in the DNA damage response (DDR) has only been addressed in a few cases, evidence for chromatin opening, nucleosome clearance and disruption of histone–DNA interactions have been reported in experimental models, notably in yeast or upon experimental induction of DNA breaks in mammals (6,11). Consistent with their important roles in the DDR, deficiencies in nucleosome remodelling may lead to defects in the repair pathways, hypersensitivity of cells to DNA damaging agents and genome instability (3,11).

Remodelling ATPases of all major families (6) are recruited to sites of DNA damage by a variety of different mechanisms (8,9). The recognition of a lesion by dedicated surveillance factors initiates signalling cascades, most prominently those mediated by the kinases Ataxia Telangiectasia mutated (ATM) and ATR (ATM and Rad3 related), which lead to local chromatin modification. The best known of such chromatin marks is the phosphorylation of histone variant H2AX at S139, also referred to as γH2AX (12,13). A considerable number of nucleosome remodelling complexes, such as the yeast INO80 and

*To whom correspondence should be addressed. Tel: +089 2180 75 427; Fax: +089 2180 75 425; Email: pbecker@med.uni-muenchen.de
Present address:
O. Mortusevicz. Gray Institute for Radiation Oncology and Biology, Department of Oncology,University of Oxford

SWR1 complexes and the mammalian SWI/SNF-type complexes can directly interact with γH2AX-containing nucleosomes [(14) and references therein]. A further early response to DNA breaks is the polymerization of ADP-ribose networks by the enzyme poly-ADP-ribose polymerase (PARP). Several remodellers are concentrated at damage sites in a PAR-dependent manner, like e.g. the chromatin remodelling enzyme ALC1 (15,16) or CHD4, the ATPase of the NURD complex (17–20).

Relatively, little is known about the functions of ISWI-type remodellers in the DDR of metazoans. These evolutionary conserved remodellers contain the ATPase ISWI (in *Drosophila*) or their vertebrate orthologues SNF2H and SNF2L. In contrast to the remodelling factors mentioned earlier, ISWI-type remodellers are not predominantly known for generating access to DNA in chromatin, but in the assembly of chromatin fibres (6). Remodelling and Spacing Factor (RSF), e.g. a complex assembled from ISWI and RSF1, is a nucleosome assembly factor as it combines histone chaperone and nucleosome spacing activities (22). In the absence of RSF complex, the DNA damage response via phosphorylation of ATM and CHK2 is compromised (23). The mammalian WICH complex, composed of SNF2H and WSTF, may associate with PCNA to assure the maintenance of chromatin structures during replication (24). Remarkably, WICH may affect the DDR by a non-remodelling mechanism as a non-canonical H2AX kinase activity was attributed to WSTF (25) and the survival of mouse embryonic fibroblasts upon challenge with MMS is reduced in the absence of WSTF (26).

We seek to understand the physiological roles of the related ISWI-type remodelling complexes CHRomatin Accessibility Complex (CHRAC) and ATP-dependent Chromatin assembly and remodelling Factor (ACF). These complexes were first identified in *Drosophila* (27,28) and subsequently found conserved in humans (21,29). CHRAC consists of ISWI (SNF2H), ACF1 and two small, histone-fold subunits, CHRAC14 and CHRAC16 (hCHRAC15 and hCHRAC17 in humans) (27,29). A complex lacking the histone-fold subunits, i.e. only consisting of ISWI/SNF2H and ACF1, is called ACF. The biochemical activities of CHRAC and ACF are very similar (30,31). CHRAC and ACF are prototypic nucleosome sliding factors; so far no nucleosome disruption activity has been detected (32,33). *In vitro*, ATP-dependent nucleosome sliding can generate 'windows of opportunity' for diverse DNA binding proteins, including nucleases and prokaryotic restriction enzymes, but also factors involved in replication, repair and recombination, to access their targets as nucleosomes are being moved (27,28,32,34–38). In addition, CHRAC/ACF can use their nucleosome sliding properties to improve the integrity of chromatin by 'spacing' nucleosomes such that gaps are closed (27,28).

The functions of CHRAC/ACF *in vivo* can be assessed by ablation of their signature subunit, ACF1. In *Drosophila*, *acf1* null mutants have a reduced viability. They display a sloppy chromatin organization with poorly distinguished eu- and heterochromatin and corresponding impairment of chromatin regulation (39,40). In human cells, depletion of hACF1 slows proliferation (41). Varga-Weisz and colleagues found that replication of heterochromatin was impaired in the absence of hACF1. Such a delay could be due to reduced chromatin opening to allow replication or to impaired chromatin assembly in the wake of the replication fork. Recently, Lan *et al.* (42) discovered that CHRAC was targeted to induced DNA breaks, where it apparently facilitates the association of the Ku70/Ku80 complex with DNA ends, a prerequisite for efficient repair.

Exploring the role of hACF1 further, we found a hitherto unappreciated involvement of hACF1 in the response of cells to diverse DNA damages. ACF1 is quickly enriched at sites of UV laser-induced damage. Interestingly, depletion of ACF1 impairs the G2/M checkpoint as a consequence of several distinct types of damaging insults: X-ray-induced DNA breaks, UV-induced pyrimidine dimers and the induction of replication forks collapse by aphidicolin. The G2/M checkpoint control senses unrepaired DNA damage and halts the progression of the checkpoint to allow time for the cell to repair the damage before entering mitosis. This process is compromised in the absence of ACF1, as cells that are challenged with the replication inhibitor aphidicolin accumulate higher levels of DSBs in the absence of ACF1. Clearly, ACF1-containing remodelling factors play a general role in the efficient response of cells to various types of DNA damage.

MATERIALS AND METHODS

Cell culture and irradiation

HeLa and U2OS cell lines were maintained at 37°C with 5% CO_2 in Dulbecco's modified Eagle's medium (DMEM, Invitrogen) supplemented with 10% foetal calf serum (FCS, Invitrogen) and penicillin/streptomycin. UV irradiation was performed in a Stratalinker (Stratagene) at doses between 10 and 1000 J/m^2. X-ray irradiation was performed with a Philips MCN-X-ray tube (250 kV, 13 mA, 2.5 + 4.0 mm Al and 1.0 mm Cu filtration) at a dose rate of 0.56 Gy/min, with final doses between 1 and 20 Gy. In both cases, cells were collected after different times of recovery.

Aphidicolin treatment and metaphase spreads

Cells were treated with 0.1 μM aphidicolin for 24 h. Colcemid (Roche) of 10 μg/ml was added 1 h before collection. Washed cells were suspended in 8 ml 75 mM KCl and incubated at 37°C for 17 min. After centrifugation, cells were fixed twice with Carnoy's fixative. Cells were spread onto a cold slide by dropping and stained with Giemsa for 2 min before washing with water. We counted obvious chromosome breaks (Figure 1B) in 50 metaphase spreads and calculated the average number per cell. The results from three independent experiments yielded the numbers presented in Figure 1C.

Plasmids, antibodies and drugs

pFPN1-ACF1-GFP and pFPN1-ACF1ΔBAZ-GFP constructs were a gift from P. Varga-Weisz (41). The

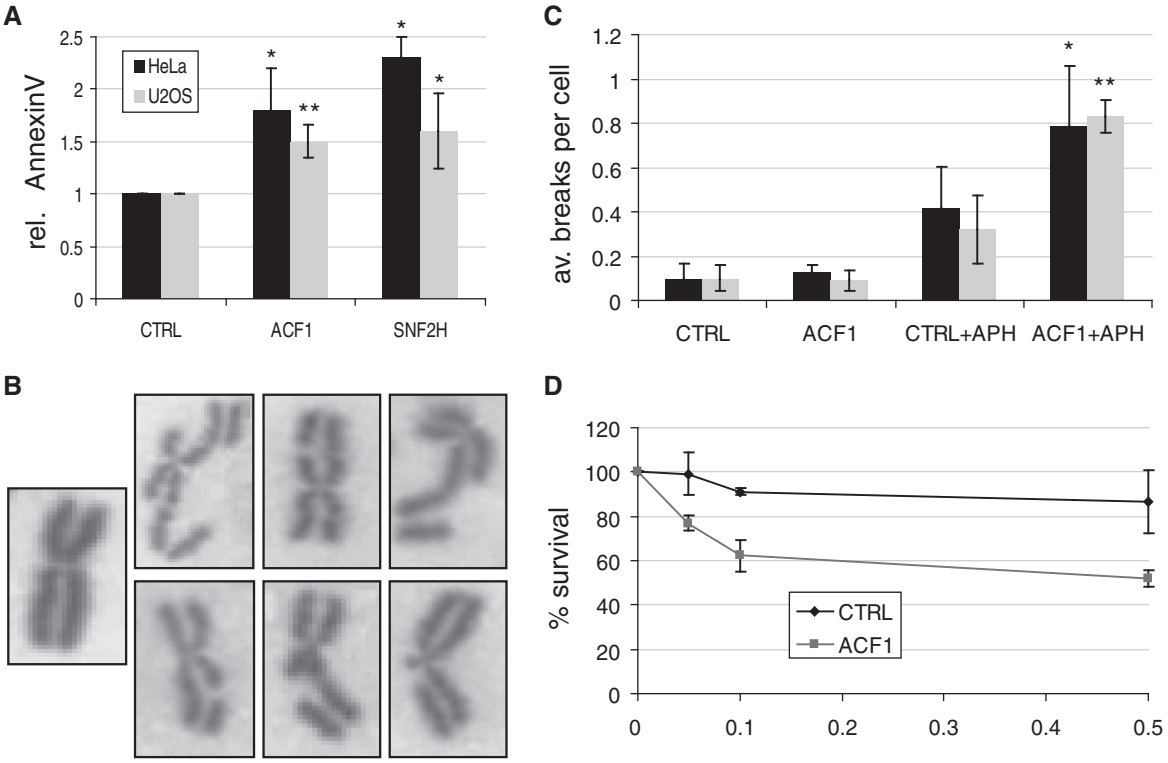

Figure 1. ACF1 depletion increases apoptosis and sensitivity to aphidicolin (APH). (**A**) Annexin V staining of U2OS and HeLa cells 72 h after transfection with siRNA1 against SNF2H or ACF1 measured by FACS analysis. PI staining allowed discarding the necrotic population. The fraction of positive cells for each condition was determined and the values normalized to the corresponding controls, which were set to 1. (**B**) Examples for metaphase chromosomes without (left) or with the types of visible breaks counted to arrive at the numbers in (C) (right). (**C**) Quantification of the number of breaks in ACF1-depleted (ACF1) and control cells (CTRL) after 24 h incubation with 0.1 μM of APH. Two different siRNA pairs where used to deplete ACF1 (black: siRNA1, grey: siRNA2). From each sample 50 cells were counted. (**D**) Clonogenic survival of HeLa cells after ACF1 depletion and controls in response to 0.05, 0.1 or 0.5 μM of APH.

pFPN1-ACF1-Ntal-GFP was constructed from the pFPN1-ACF1-GFP plasmid by cutting with ScaI and BamHI before the WACZ domain and before GFP sequence, respectively. The ends were filled in with Klenow polymerase and ligated. This construct contains the N terminus including the BAZ domain, but lacks the WACZ, PHD and bromodomains. The following antibodies were used: ACF1 (Bethyl Laboratories A301-318 A); WSTF (Epitomics 2033-1); SNF2H (E. Kremmer, HelmholtzZentrum, Münich); CHK2T68ph (Cell Signalling 2661); tubulin (SIGMA T9026); γH2AX (Millipore 05-636); H3S10ph (Millipore 05-806); ATMS1981ph (Cell Signalling 4526) and ATM (Abcam ab32420).

siRNA and DNA transfections

Target sequences for small interfering (si)RNAs are described in Table 1. The small duplexes (MWG) were introduced with Oligofectamine and Optimem (Invitrogen) according to the supplier's protocol. Cells at 40–50% confluency were transfected with 200 pmol siRNA and were collected 72 h later. For transient transfections of GFP constructs with the Jetpei reagent (Peqlab), cells at 70–80% confluency were transfected with 1–2 μg of plasmid according to the manufacturer's specifications and samples were collected 48 h later.

Table 1. siRNA sequences for RNA interference

Target	Sequence
ACF1 siRNA1	CAC UGU GAA CCA CAA GAU G
ACF1 siRNA2	TTA CAT GAG TCT GCT ATT G
SNF2H siRNA1	GAG GAG GAU GAA GAG CUA U
SNF2H siRNA2	UGA CAA GGG UAU UGG ACA U
WSTF	GAA CAG GAA GUU GCU GAG C
CTRL siRNA1	CUU ACG CUG AGU ACU UCG A
CTRL siRNA2	CGU ACG CGG AAU ACU UCG A

Clonogenic assays

Colony formation assays were performed as described (43). In short, cells were transfected at Day 0, trypsinized and replated in defined numbers on Day 2 and irradiated 3 h later. Appropriate cell numbers were seeded in triplicates. The plates were collected on Day 10, stained with 80% EtOH, 0.3% methylene blue and washed three times with water. Colonies containing >50 cells were counted microscopically.

Cell extract preparation and western blotting

Whole-cell extracts from 2 to 3×10^6 cells were prepared in IPH buffer (50 mM Tris–HCl pH 8, 150 mM NaCl,

5 mM EDTA, 0.5% NP-40) containing protease and phosphatase inhibitors (Sigma). Cells were kept on ice for 10 min followed by centrifugation at 13 krpm for 10 min at 4°C. Protein concentration was analysed with Bradford Reagent (Biorad). For western blot analysis, boiled protein in sample buffer was separated on 7–15% acrylamide gels and transferred to Protran nitrocellulose membranes (Whatman). Incubation with primary antibodies was at 4°C overnight. Secondary antibodies were compatible with IR fluorescence detection on a LI-COR Odyssey® Infrared Imaging System at medium intensities.

Immunofluorescence

Cells on cover slips were fixed in 4% paraformaldehyde-PBS for 20 min and permeabilized with methanol for 10 min. Alternatively, cells were fixed in 3.7% formaldehyde and permeabilized with 0.5% Triton X-100 in PBS for 5 min. After blocking with 3% bovine serum albumin (BSA) in PBS with 0.1% Triton X-100 (PBST) for 30 min, cells were incubated for 2 h in primary antibody diluted into 3% BSA in PBST. After three washes with PBST cells were incubated for 1 h with CY3 or Alexa488 labelled secondary antibodies. Cells were mounted onto a slide with Vectashield (Vector Laboratories) containing DAPI (4′,6′-diamidino-2-phenylindole). Confocal images (512 × 512 pixels) from three different channels were collected with a Leica SP5 microscope equipped with a Plan-Apochromat 63×/1.4 oil immersion objective.

Flow cytometry

Apoptotic cells were detected with an Annexin V Apoptosis Detection Kit (Biovision). Cells (1.5×105) were collected by centrifugation and suspended in 0.5 ml of buffer containing calcium. Annexin V-conjugated with FITC and PI were added to the sample, which was incubated at room temperature (RT) for 5 min in the dark. The percentage of Annexin V-FITC positive cells without PI staining was determined and normalized to the control cells. To measure H3S10ph, cells were washed twice in PBS, fixed in 70% ethanol for 1 h at −20°C and stained with a 1:100 dilution of the primary antibody for 2 h at RT. After washing, cells were incubated for 1 h at RT in the dark with Alexa488-conjugated secondary antibody. DNA staining for analysis of cell cycle phases was done with cells fixed in 70% ethanol for 1 h at −20°C using 25 µl PI (1 mg/ml) and 5 µl RNase (10 mg/ml). To analyse cells with subG1 DNA content the culture was harvested 96 h after siRNA treatment. Data were collected with BD FACSCANTO and analysed with BD FACSDIVA software (BD Biosciences).

Live-cell microscopy and laser microirradiation

Live cell imaging and micro-irradiation experiments were carried out with a PerkinElmer UltraView Vox spinning disk microscope equipped with a Plan-Apochromat 63×/1.4 oil objective using Volocity software 5.3 for image capturing. GFP and RFP were excited with 488 nm and 561 nm DPSS laser lines, respectively. The microscope was equipped with a heated environmental chamber set to 37°C. Confocal image series were typically recorded with a frame size of 256 × 256 pixels and a pixel size of 109 nm.

For localized DNA damage induction, cells were seeded in µ-slides VI or gridded µ-dishes (ibidi) and sensitized by incubation in DMEM supplemented with 10% FCS and 50 µg/ml gentamicin-containing BrdU (10 µg/ml) for 24–48 h at 37°C. Prior to live-cell imaging, the medium was changed to phenol-red-free medium containing 25 mM HEPES. Micro-irradiation was performed using the FRAP preview mode of the Volocity software by repeatedly scanning (1200 iterations) a preselected stripe (18×0.5 µm) within the nucleus with a 405 nm diode laser set to 50 µW, which leads to generation of a detectable DDR in a pre-sensitization-dependent manner. The laser power was measured after passing through the objective lens with a laser power meter (Coherent). Before and after micro-irradiation confocal image series of one mid z-section were recorded at 2 s time interval (typically 6 pre-irradiation and 150 post-irradiation frames). For evaluation of the recruitment kinetics, fluorescence intensities at the irradiated region were corrected for background and for total nuclear loss of fluorescence over the time course and normalized to the pre-irradiation value. For the quantitative evaluation of micro-irradiation experiments, data of at least 10 nuclei were averaged and the mean curve and the standard error of the mean calculated and displayed using Microsoft Excel software.

Statistical analysis

All quantifications are based on three independent experiments. For every sample, the mean value and error bars, representing the standard deviation, are calculated. For analyses of significance a two-tailed Fisher's exact test was used with the exception of the analysis of Supplementary Figure S5B, for which a one-tailed test was employed and *P*-values represented with one asterisk (*) if $P < 0.05$, two (**) if $P < 0.01$ and three (***) if $P < 0.001$.

RESULTS

ACF1 depletion leads to apoptosis

Depletion of ACF1, the signature subunit of CHRAC/ACF complexes, was previously shown to impair proliferation in HeLa cells (41). We confirmed these results in HeLa and U2OS cells, in which expression of hACF1 and the associated SNF2H ATPase subunit can be efficiently reduced by RNA interference (44). Two days after transfection of small-interfering RNA duplex oligonucleotides (siRNA) ACF1 expression was already strongly reduced (Supplementary Figure S1A). After 3 days the ACF1 knockdown led to reduced proliferation of HeLa cells when compared to a parallel culture treated with control siRNA (Supplementary Figure S1B). Depletion of the ATPase SNF2H resulted in a similar proliferation defect (Supplementary Figure S1A and S1B), which is in agreement with the previously suggested role for these proteins in replication (41,45). In either case, the expression of the related WSTF was unaffected (Supplementary

Figure S1C). However, we also observed increased cell death in the cultures that were depleted of SNF2H or ACF1. We quantified the binding of fluorescent Annexin V to accessible phosphatidylserine in the outer cell membrane by cytometry, as a measure of early apoptotic events. Annexin V levels were increased in U2OS and HeLa cells when ACF1 or SNF2H were depleted (Figure 1A and Supplementary Figure S1D). Similar increases were seen if the remodeller subunits were depleted with a second pair of siRNA oligonucleotides, excluding a dominant off-target effect (Supplementary Figure S1D and S1E). The apoptotic phenotype was confirmed by fluorescence-activated cell scanning (FACS), measuring the DNA content by propidium iodide (PI) staining. Cells with reduced expression of ACF1 or SNF2H showed enhanced cell fragmentation as a marker of late apoptosis, indicated by cells with lower than G1 DNA content (Supplementary Figure S1F and data not shown). It is known that SNF2H is required for viability *in vivo* (46) and that depletion of SNF2H in tissue culture cells leads to apoptosis (25), yet it was unexpected that depletion of ACF1 had similar consequences. An increased apoptosis rate may indicate an accumulation of DNA damage due to increased replication defects, compromised repair or incomplete checkpoint activation. These possibilities led us to explore the consequences of reduced ACF1 levels after DNA damage induction.

Depletion of ACF1 increases aphidicolin-induced chromosomal fragility

Varga-Weisz and colleagues (41) suggested that the depletion of ACF1 leads to a delay in the later stages of replication. Partial inhibition of DNA polymerase α with aphidicolin is known to particularly affect late replication: in the presence of the inhibitor some late replicating chromosomal areas may end up not being replicated, which leads to visible breaks in metaphase chromosomes, also known as 'fragile sites' (47–51). We therefore tested whether ACF1 depletion increases the aphidicolin-induced replication stress by monitoring metaphase chromosome breaks. HeLa cells were incubated with 0.1 μM aphidicolin for 24 h treated with colcemid and metaphase spreads were visually inspected for chromosome breaks (Figure 1B). Depletion of ACF1 with two different siRNAs led to a significant increase in the number of chromosome breaks, when compared to the RNAi control (Figure 1C). In the absence of aphidicolin, only very few breaks were observed and the number of breaks were not increased if ACF1 was depleted. This may indicate that depletion of ACF1 does not lead to replication fork collapse itself, but diminishes the recovery from such damage. In support of this idea, the survival of HeLa cells challenged with aphidicolin at concentrations between 0.05 and 0.5 μM is strongly reduced upon depletion of ACF1 (Figure 1D). Treatment of cells with aphidicolin can induce intra-S and G2/M checkpoints (50). The incubation of HeLa cells with 0.1 μM aphidicolin generated chromosome breaks without noticeable alterations in the cell cycle, but higher doses of the inhibitor lead to S-phase arrest, which is not modified by ACF1 knockdown (data not shown). U2OS cells mount a G2/M arrest at low doses of aphidicolin and accumulate high levels of damage in metaphase chromosomes (Figure 2A and data not shown). In the absence of ACF1, an increased number of S phase intermediates were observed and at the same time the G2/M peak was diminished (Figure 2A). In order to discriminate between cells in G2 and M phases, we combined PI staining with staining for histone H3 phosphorylated at serine 10 (H3S10ph), a chromatin mark for mitotic cells (52). Whereas aphidicolin treatment decreases the percentage of mitotic cells after G2/M checkpoint activation in control cells, this population is increased significantly after ACF1 knockdown (Figure 2B and C), indicating that ACF1 is required for proper checkpoint activation.

ACF1 modulates the response of cells to damaging radiation

Our data documented a role for ACF1 in the response to replication-associated DNA breaks, which raised the question as to whether ACF1 was also involved in the cellular response to other types of damage. In support of this hypothesis, Lan *et al.* (42) recently reported that ACF1 is involved in the repair of X-ray-induced DNA breaks. In an independent, parallel effort, we explored the relationship between ACF1 and the response of cells to UV- and X-rays. U2OS cells, in which ACF1 had been depleted for 48 h, and appropriate controls were irradiated with different doses of UV- and X-rays and their survival was monitored in a clonogenic assay (Supplementary Figure S2A). Our data confirm and complement the ones of Lan *et al.* (42). At doses of X-ray below 3–4 Gy the depletion of ACF1 has a minor effect on cell survival [Supplementary Figure S2A, (42)]. ACF1-depleted cells show an increased sensitivity against higher doses of X-ray (6 and 9 Gy) (42). Lan *et al.* (42) concluded that the sensitivity of cells towards low doses of UV irradiation (up to 10 J/m^2) was not severely affected, but we found a moderate sensitization at higher doses of UV (Supplementary Figure S2A). In order to confirm these results, we used apoptosis as a surrogate marker for cell viability at high irradiation doses. HeLa and U2OS cells were irradiated with 100 J/m^2 or 10 Gy, allowed to recover for 24 h and stained for Annexin V to monitor apoptosis. Cells with reduced ACF1 levels showed increased apoptosis in response to both, UV- and X-ray (Supplementary Figure S2B).

Since several of the known nucleosome remodelling factors are directly recruited to sites of radiation damage (15,17,53), we wished to characterize ACF1 in this respect. Local DNA damage was introduced into BrdU-sensitized HeLa cells by micro-irradiation with a 405 nm laser. The track of DNA damage was marked by a line of diagnostic γH2AX modification. We found that endogenous ACF1 quickly localized to laser-induced DNA lesions colocalizing with the damage marker γH2AX (Figure 3A). In addition we detected recruitment of the ACF1 ATPase partner SNF2H to laser-induced DNA damage sites, as well as recruitment of the ACF1-related WSTF (Supplementary Figure S3A), which had been proposed to be necessary for the long-term maintenance of γH2AX (25). To analyse the *in vivo* kinetics of ACF1 recruitment,

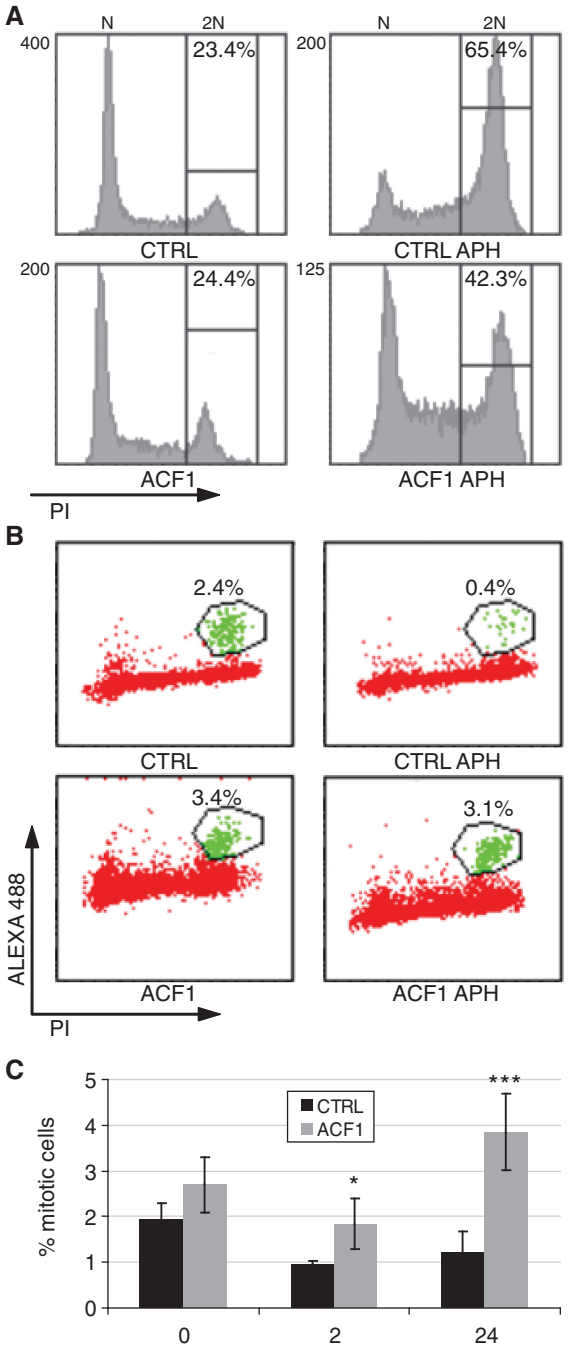

Figure 2. ACF1 depletion compromises the G2/M checkpoint after APH treatment. (**A**) Control U2OS cells (CTRL) or cells depleted of ACF1 (ACF1) by treatment with siRNAs for 72 h were incubated with 0.3 μM APH for 24 h. Cells were harvested, fixed and the cell cycle distribution was analysed by DNA staining with PI. (**B**) Control cells (CTRL) or ACF1-depleted U2OS cells (ACF1) were incubated for 24 h with 0.3 μM APH. Cells were sorted by DNA content (PI staining) and the mitosis marker H3S10ph. Double-positive cells are labelled by green dots. (**C**) Quantification of mitotic cells for U2OS upon ACF1 knockdown after incubation of 2 h with 1 μM or 24 h with 0.3 μM APH.

we transiently expressed GFP-tagged ACF1 together with RFP-PCNA as a positive control and followed the real-time accumulation of both proteins after damage induction in living cells. We found that ACF1-GFP, like PCNA, accumulated at DNA damage sites within 30 s after irradiation (54) (Figure 3B and Supplementary Figure S3B). The C-terminus of ACF1, containing the PHD and bromodomain modules, was not required for efficient recruitment. Interestingly, the N-terminal fragment of ACF1 showed an even faster accumulation than the full length ACF1 (Figure 3C and D). This change in the $t_{1/2}$ might be due to a weaker retention of the protein at other chromatin targets leading to faster redistribution. The recruitment of the N-terminal part of ACF1 can be explained by the presence of several potential targeting surfaces, such as the BAZ domain that mediates the SNF2H interaction (41) and an interaction surface for the CHRAC17/CRAC15 subunits (31). An additional potential DNA binding determinant had been observed for the *Drosophila* ACF1 homolog in the ACF1 N terminus (55). ACF1-GFP and SNF2H-GFP accumulated with very similar kinetics (Supplementary Figure S3B and S3C). In order to test, to which extent ACF1 recruitment depends on the SNF2H interaction we expressed a protein lacking the BAZ domain, which mediates the SNF2H interaction (ACF1-ΔBAZ) (41). Deletion of the BAZ domain led to a significant decrease in ACF1 recruitment (Figure 3C and D). This highlights an important, but not exclusive, contribution of the SNF2H interaction for ACF1 recruitment. Our data are in good agreement with recent findings that SNF2H and ACF1 accumulate at UV laser-induced tracks of damaged chromatin in U2OS cells (42,56).

The radiation-induced G2/M checkpoint is incomplete in the absence of ACF1

The above-mentioned data firmly establish a role for ACF1 in the cellular response to radiation damage. The observation that ACF1 depletion compromised the G2/M checkpoint after replication stress prompted us to test whether ACF1 also plays a role in G2/M checkpoint activation after UV/X-ray irradiation. ACF1-depleted HeLa cells were irradiated with X-rays at 10 Gy and the cell cycle distribution was monitored after different time points by FACS analysis. Control cells showed a profound G2/M arrest, which was moderately reduced after ACF1 knockdown (Figure 4A). In order to discriminate between cells in G2 and M phases we combined PI staining with staining for histone H3S10ph as before. Control HeLa cells or ACF1-depleted cells were irradiated with UV (100 J/m^2) or X-ray (1 Gy). The quantification of the mitotic fraction of control cells revealed a clear reduction after both UV and X-ray irradiation, as expected from an intact G2/M checkpoint arrest (Figure 4B). Remarkably, upon depletion of ACF1 up to 2-fold more mitotic cells were observed, suggesting that the G2/M checkpoint was not properly activated particularly after short recovery times (Figure 4C and D). The same results were obtained with U2OS cells and using two different siRNAs against ACF1 (Supplementary Figure S4A and S4B, respectively). Most proteins involved in checkpoint activation are individually dispensable for a proper arrest at high levels of damage when more than one repair/signalling pathway is active (59). However, we found more mitotic cells in the absence of ACF1 even at much higher

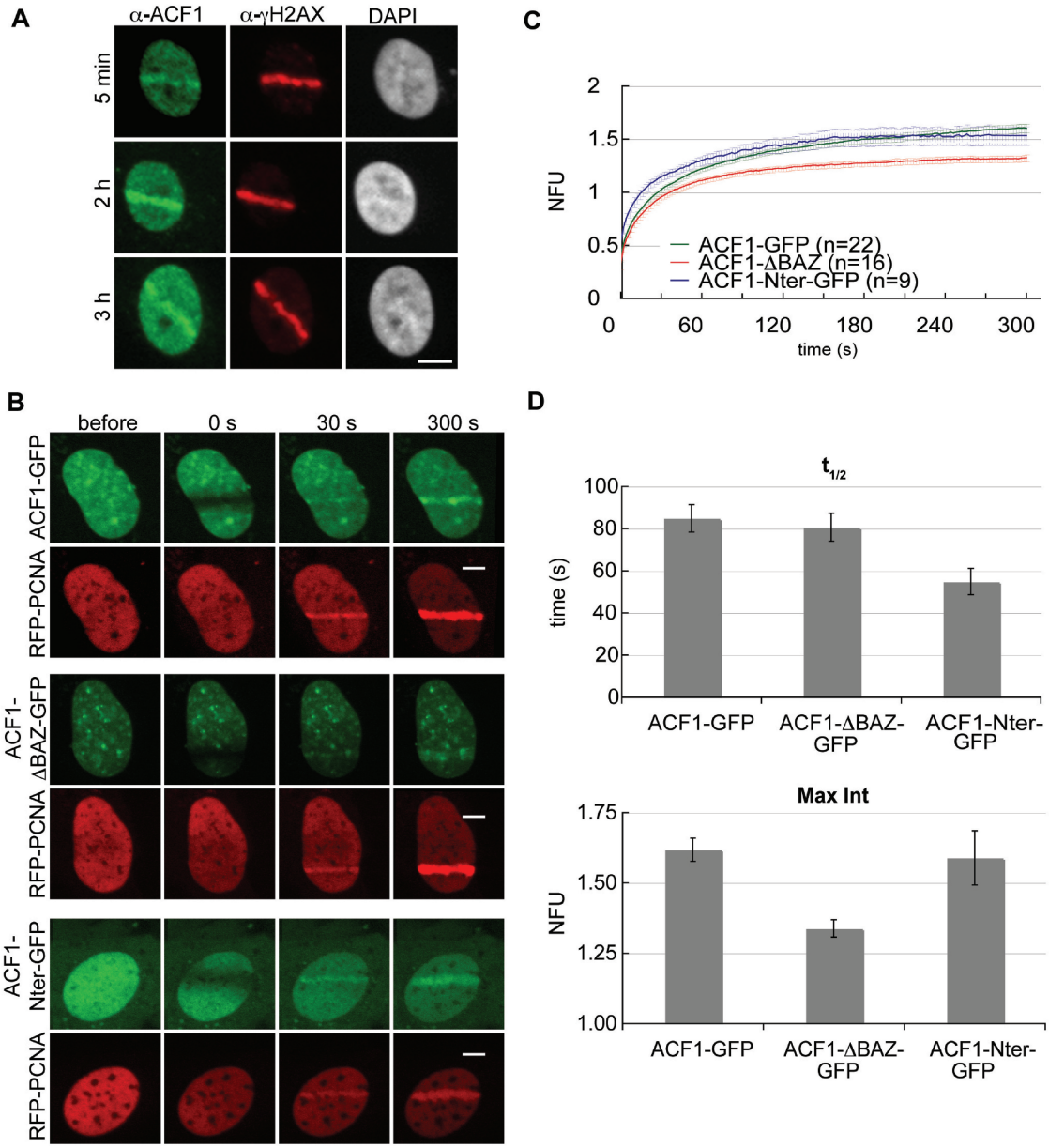

Figure 3. Recruitment of ACF1 to laser-induced DNA damage sites. (**A**) Endogenous ACF1 accumulates at laser-induced DNA damage sites. Confocal images of HeLa cells fixed at indicated time points after laser micro-irradiation and stained for ACF1 and the DNA damage marker γH2AX are shown. (**B**) Live imaging of MEFs expressing either full-length ACF1 (ACF1-GFP), a deletion construct missing the BAZ domain (ACF1-ΔBAZ-GFP) or the N-terminal part of ACF1 (ACF1-Nter-GFP) together with RFP-PCNA. (**C**) Quantitative evaluation of recruitment kinetics shown in (B). (**D**) Graphs showing the halftime of recruitment ($t_{1/2}$), which is the time needed for reaching half of the final intensity at the micro-irradiated area and the Max Int, which is the final intensity at the micro-irradiated area reached within the observation period of 5 min, for the indicated ACF1 fusion proteins. Scale bar, 5 μm.

irradiation doses (1000 J/m^2 UV and 10 Gy X-rays; Supplementary Figure 4C). Interestingly, in contrast to the results obtained after ACF1 knockdown, depletion of WSTF (Supplementary Figure S1C), the non-catalytic subunit of the WICH complex, which is involved in signal transduction upon DSB induction (25), leads to reduced rather than increased numbers of mitotic cells (Figure 4C and D). Apparently, ACF1-containing remodellers, but not the WICH complex, contribute to activating the G2/M checkpoint arrest.

One of the main markers of DNA damage, phosphorylation of H2AX at serine 139 (γH2AX), is necessary for signal amplification upon DNA damage but dispensable for initial recognition of the damage (58). To further investigate the role of ACF1 in G2/M checkpoint activation, we analysed γH2AX levels in ACF1-depleted cells that were damaged in various ways. In support of our previous results, ACF1 depletion led to reduced levels of γH2AX after aphidicolin treatment and irradiation (Figure 5A), even allowing for 24 h of recovery after X-ray irradiation (Supplementary Figure S5A). ATMS1981ph and CHK2T68ph are two phosphorylation marks that characterize the G2/M checkpoint (12,57,52). While we observed a reduction of CHK2T68ph upon

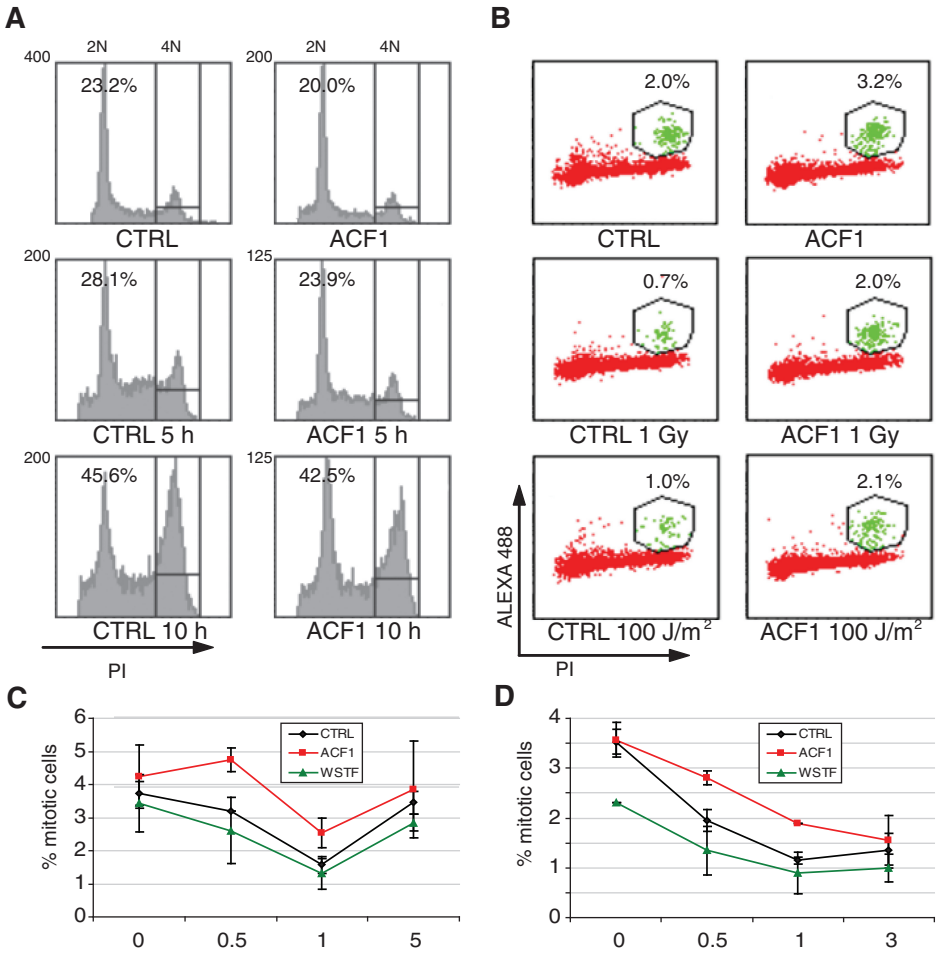

Figure 4. ACF1 depletion compromises the G2/M checkpoint after irradiation. (**A**) HeLa cells were treated with siRNAs for 72 h and irradiated with 10 Gy. Cells were allowed to recover for 5 or 10 h. They were collected, ethanol fixed and the cell cycle distribution was analysed by PI staining for DNA content. (**B**) Cell cycle distribution of HeLa cells depleted for ACF1 in comparison to controls 1 h after irradiation with 1 Gy or 100 J/m^2. Cells were sorted by DNA content (PI staining) and the mitosis marker H3S10ph. Double-positive cells are labelled by green dots. (**C**) Time course analysis of mitotic cells (marked green in B) after knockdown of ACF1 or WSTF and irradiation of cells with 100 J/m^2. (**D**) The same as in (C) with 1 Gy X-ray irradiation.

ACF1 depletion, ATMS1981ph appeared hardly affected, considering that a slight overall reduction of ATM levels cannot be excluded (Figure 5B). In order to quantify and provide a measure of reproducibility, we performed additional X-ray irradiation experiments with varying doses and 1 h of recovery and quantified the resulting western blots using a LI-COR Odyssey® Infrared Imaging System. The band intensities from triplicates were normalized to the tubulin signals in the same lane (Figure 5C). The data show a clear reduction of the γH2AX signal in ACF1-depleted cells. We also attempted to obtain independent confirmation for the reduction by staining cells with antibodies against γH2AX after UV- and X-ray irradiation and measuring the mean intensity of the population by FACS. ACF1 depletion yields a modest decrease in the intensity of γH2AX, although at this depth of analysis the data merely illustrate a trend (Supplementary Figure S5B). Direct visualization of immunofluorescence staining of γH2AX yields qualitative support (Supplementary Figure S5C). In summary, our results demonstrate that at reduced ACF1 levels the signaling of DNA damage is impaired.

In their parallel effort, Lan *et al.* (42) counted the number of foci per cell or the number of cells with foci at different times after irradiation and observed an increase of γH2AX foci after longer recovery times (24–48 h). Conceivably, the persistence of γH2AX foci reflect the function of ACF1 in repair, whereas the reduction of overall γH2AX levels early reflect its involvement in the initial signalling that sets the G2/M checkpoint.

DISCUSSION

ACF1 and checkpoint control

Probing the integrity of the G2/M checkpoint in the context of replication fork collapse, UV-induced pyrimidine dimers and X-ray-induced DSB we found diminished checkpoint activation in the absence of ACF1. Entering mitosis with unrepaired DNA lesions due to a faulty

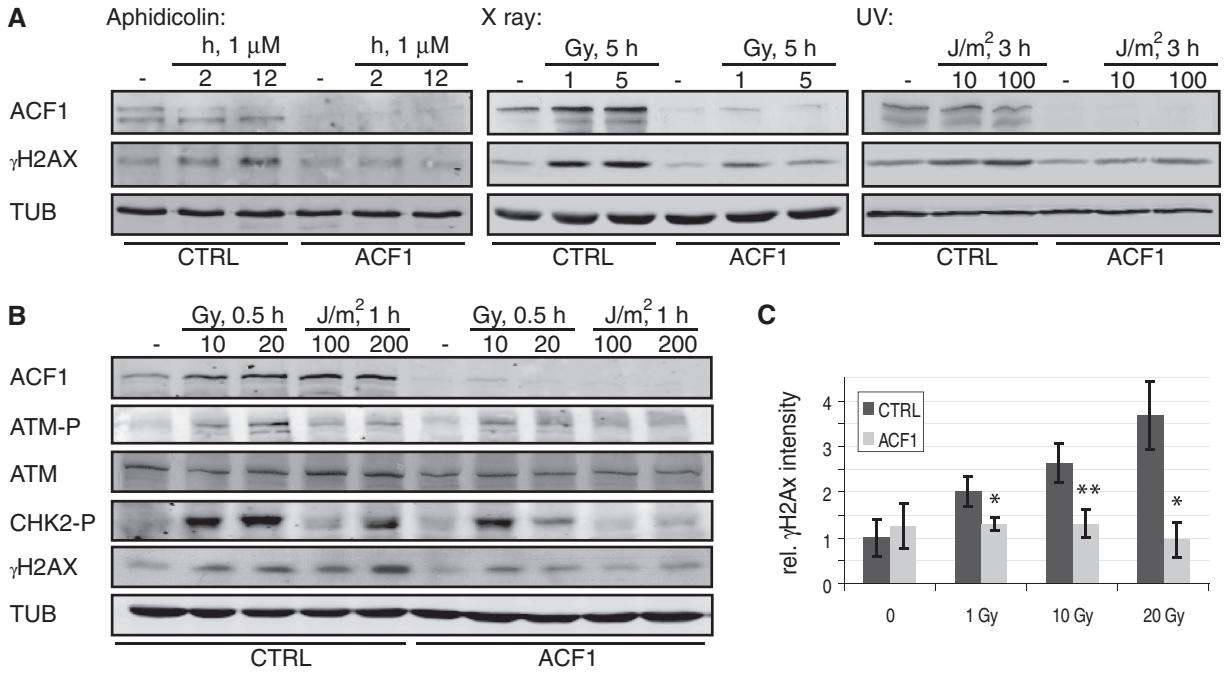

Figure 5. ACF1 depletion diminishes H2AX, CHK2 and ATM phosphorylation. (**A**) ACF1-depleted HeLa cells and controls received the following treatments: 1 μM APH for 2 or 12 h; X-ray irradiation for 1 or 5 Gy followed by recovery of 5 h; UV irradiation with 10 or 100 J/m^2 and recovery for 3 h. Whole-cell extracts were prepared and ACF1, γH2AX and tubulin levels were detected by western blotting. (**B**) ACF1-depleted HeLa cells were irradiated as indicated and processed as in (A) for visualisation of the indicated antigens described fully in the text. (**C**) Quantification of γH2AX by western blotting on a LI-COR Odyssey® Infrared Imaging system after irradiation of the indicated doses of X-ray and 1 h of recovery. Band intensities are normalized to the loading control tubulin and relative to the control without irradiation.

G2/M checkpoint can have severe consequences as this may lead to generation of more damage, chromosome breaks, aneuploidy or malignant transformation (60,61). We showed the increased number of DNA breaks in metaphase chromosomes in the absence of ACF1 after inducing replicative stress with aphidicolin. So far, the only known molecular context for ACF1 is the association with the ATPase SNF2H in the nucleosome remodelling factors ACF and CHRAC. We conclude that ACF1—and by inference the remodelling factors it defines—is involved in the cellular response to several distinct types of DNA lesions. Interestingly, unbalanced expression of another SNF2H interactor, RSF1, can lead to DNA breaks and chromosome instability (23). It is unknown, whether different SNF2H interactors compete with the common ATPase and whether an increase of RSF would lead to reduced CHRAC/ACF complexes.

While this manuscript was in preparation, Lan *et al.* (42) described a role for ACF/CHRAC in DSB repair. Their data suggested that ACF1 facilitates the loading of the KU complex to chromosomal breakpoints, but did not address the consequences for checkpoint arrest. In this context, our finding of an impaired G2/M arrest upon depletion of ACF1 has important implications. Depletion of repair factors usually leads to an increase in the G2/M checkpoint. For example, it has been suggested that KU80 deficiency in mammalian cells or KU70 in yeast leads to stronger G2/M checkpoint (62,63). Apparently, ACF1 contributes to both processes: repair and checkpoint activation. The combined loss of these functions is expected to lead to dramatic consequences, as continued proliferation in the presence of DNA damage predisposes cells for chromosomal instability and malignant translocations (60,61). However, consistent with the known roles for nucleosome remodelling factors as facilitators of chromosomal interactions rather than primary targeting determinants the contributions of ACF1 appear modulatory, rather than decisive.

In the context of DSB repair, interactions between ACF1 and KU70 were recently shown to be important. In the absence of ACF1, reduced levels of KU70/80 were found at DSB (42). The checkpoint defects we found here cannot be explained by reduced KU loading since this would normally lead to a hyperactive G2/M arrest (62,63). Furthermore, KU is not involved in the repair of pyrimidine dimers or coping with replication stress. Therefore, we speculate that ACF1 has a broader role in promoting the G2/M checkpoint in response to diverse types of DNA damage and it will be interesting to dissect its role in these diverse scenarios.

Targeting ACF

The different recruitment kinetics of repair proteins to DNA lesions provide a first indication on their respective role in the DDR. The fast and early recruitment of ACF1 to sites of laser-induced lesions parallels that of the sliding clamp PCNA. This is unlikely to be due to direct interaction with PCNA (24), but may at least in part be

explained by direct binding to the KU complex (42). This early recruitment supports our hypothesis that ACF1 acts upstream of the checkpoint signalling marks γH2AX and phospho-CHK2. In yeast the presence of the γH2AX modification serves as a reference for the approximate timing of factor recruitment. A number of remodelling complexes have been described to accumulate at lesion sites before or after the appearance of γH2AX (8). For instance, RSC is recruited rapidly, although still slower than mammalian ACF1, during the first 10 min after damage induction (64) and it has been proposed to be responsible for H2AX phosphorylation along with SWI/SNF. This is in contrast to the Ino80 complex, whose recruitment depends on prior γH2AX modification (65,66). However, not all remodellers that are recruited to the lesion site early play similar roles. For example, the mammalian SWI/SNF complex is recruited to DSBs early and is involved in stimulating the phosphorylation of H2AX, but depletion of critical subunits had no effect on the establishment of the G2/M checkpoint (67,53).

The dichotomy in the relationship between remodellers and the G2/M checkpoint is perhaps best illustrated by our experiment, in which we depleted cells in parallel of either ACF1 or the related WSTF protein, which associates with SNF2H to form the WICH complex (24,25,45). Depletion of WSTF leads to a stronger G2/M checkpoint, whereas ACF1 depletion renders the checkpoint leaky.

A global role for ACF1 in the DNA damage response?

The role of ACF1 in the DDR we identified here is reminiscent of the CHD4-containing NuRD complex, which is recruited within 30 s after micro-irradiation and is required for an intact G2/M checkpoint (18,19). CHD4 depletion affects the levels of RNF168-dependent ubiquitination at lesion sites, which presumably has many substrates. The identification of more functional and physical interactors of ACF1 will help to elucidate the role of ACF1 in the damage response pathway. The fact that ACF1 is required for loading of the KU complex onto DSBs is in line with its biochemical property to render DNA accessible by nucleosome sliding (27,28,32,34–38). However, such a role has not yet been documented *in vivo*. Loss- and gain-of-function studies of ACF1 in *Drosophila* suggest a role for ACF1-containing remodellers in the assembly of intact chromatin fibres as a prerequisite for higher order chromatin organization (39,40). Therefore, we also consider a role for CHRAC/ACF as a repair factor specialized to deal with the chromatin aspect of the repair process. Any repair of the damaged DNA needs to be followed by reconstitution of chromatin integrity. The known biochemical properties of CHRAC/ACF in nucleosome assembly and nucleosome spacing are perfectly suited to fulfill the task of chromatin fibre repair. It will be interesting to explore, whether persistent defects at the level of chromatin organization can be sensed to delay cell cycle progression.

SUPPLEMENTARY DATA

Supplementary Data are available at NAR Online.

ACKNOWLEDGEMENTS

We thank P. Varga-Weisz for SNF2H and ACF1 expressing plasmids, O. Fernandez-Capetillo and N. Agell for helpful discussions and S. Bohlander for help with metaphase spreads.

FUNDING

Deutsche Forschungsgemeinschaft (SFB648 and Be1140/6-1 to P.B.B., SFB646 and SFB684 to H.L.); Cluster of Excellence 'Munich-Centre for Advanced Photonics' (to A.A.F.); Nanosystems Initiative and the BioImaging Network Munich (to H.L.); MD Program 'Molecular and Systemic Medicine of the Medical Faculty (to B.B.). Funding for open access charge: Grant from the Deutsche Forschungsgemeinschaft.

Conflict of interest statement. None declared.

REFERENCES

1. Sharma,G.G., So,S., Gupta,A., Kumar,R., Cayrou,C., Avvakumov,N., Bhadra,U., Pandita,R.K., Porteus,M.H., Chen,D.J. *et al.* (2010) MOF and histone H4 acetylation at lysine 16 are critical for DNA damage response and double-strand break repair. *Mol. Cell. Biol.*, **30**, 3582–3595.
2. Downs,J.A. (2008) Histone H3 K56 acetylation, chromatin assembly and the DNA damage checkpoint. *DNA Repair*, **7**, 2020–2024.
3. Downs,J.A., Nussenzweig,M.C. and Nussenzweig,A. (2007) Chromatin dynamics and the preservation of genetic information. *Nature*, **447**, 951–958.
4. Wurtele,H. and Verreault,A. (2006) Histone post-translational modifications and the response to DNA double-strand breaks. *Curr. Opin. Cell Biol.*, **18**, 137–144.
5. van Attikum,H. and Gasser,S.M. (2005) The histone code at DNA breaks: a guide to repair? *Nat. Rev. Mol. Cell Biol.*, **6**, 757–765.
6. Clapier,C.R. and Cairns,B.R. (2009) The biology of chromatin remodeling complexes. *Annu. Rev. Biochem.*, **78**, 273–304.
7. Korber,P. and Becker,P.B. (2010) Nucleosome dynamics and epigenetic stability. *Essays Biochem.*, **48**, 63–74.
8. van Attikum,H. and Gasser,S.M. (2005) ATP-dependent chromatin remodeling and DNA double-strand break repair. *Cell Cycle*, **4**, 1011–1014.
9. Bao,Y. and Shen,X. (2007) Chromatin remodeling in DNA double-strand break repair. *Curr. Opin. Genet. Dev.*, **17**, 126–131.
10. Jackson,S.P. and Bartek,J. (2009) The DNA-damage response in human biology and disease. *Nature*, **461**, 1071–1078.
11. Osley,M.A., Tsukuda,T. and Nickoloff,J.A. (2007) ATP-dependent chromatin remodeling factors and DNA damage repair. *Mutat. Res.*, **618**, 65–80.
12. Sancar,A., Lindsey-Boltz,L.A., Unsal-Kacmaz,K. and Linn,S. (2004) Molecular mechanisms of mammalian DNA repair and the DNA damage checkpoints. *Annu. Rev. Biochem.*, **73**, 39–85.
13. Fernandez-Capetillo,O., Lee,A., Nussenzweig,M. and Nussenzweig,A. (2004) H2AX: the histone guardian of the genome. *DNA Repair*, **3**, 959–967.
14. Lee,H.S., Park,J.H., Kim,S.J., Kwon,S.J. and Kwon,J. (2010) A cooperative activation loop among SWI/SNF, gamma-H2AX and H3 acetylation for DNA double-strand break repair. *EMBO J.*, **29**, 1434–1445.
15. Ahel,D., Horejsi,Z., Wiechens,N., Polo,S.E., Garcia-Wilson,E., Ahel,I., Flynn,H., Skehel,M., West,S.C., Jackson,S.P. *et al.* (2009) Poly(ADP-ribose)-dependent regulation of DNA repair by the chromatin remodeling enzyme ALC1. *Science*, **325**, 1240–1243.
16. Gottschalk,A.J., Timinszky,G., Kong,S.E., Jin,J., Cai,Y., Swanson,S.K., Washburn,M.P., Florens,L., Ladurner,A.G.,

Conaway,J.W. *et al*. (2009) Poly(ADP-ribosyl)ation directs recruitment and activation of an ATP-dependent chromatin remodeler. *Proc. Natl Acad. Sci. USA*, **106**, 13770–13774.
17. Polo,S.E., Kaidi,A., Baskcomb,L., Galanty,Y. and Jackson,S.P. (2010) Regulation of DNA-damage responses and cell-cycle progression by the chromatin remodelling factor CHD4. *EMBO J.*, **29**, 3130–3139.
18. Larsen,D.H., Poinsignon,C., Gudjonsson,T., Dinant,C., Payne,M.R., Hari,F.J., Danielsen,J.M., Menard,P., Sand,J.C., Stucki,M. *et al*. (2010) The chromatin-remodeling factor CHD4 coordinates signaling and repair after DNA damage. *J. Cell. Biol.*, **190**, 731–740.
19. Smeenk,G., Wiegant,W.W., Vrolijk,H., Solari,A.P., Pastink,A. and van Attikum,H. (2010) The NuRD chromatin-remodeling complex regulates signaling and repair of DNA damage. *J. Cell. Biol.*, **190**, 741–749.
20. Chou,D.M., Adamson,B., Dephoure,N.E., Tan,X., Nottke,A.C., Hurov,K.E., Gygi,S.P., Colaiacovo,M.P. and Elledge,S.J. (2010) A chromatin localization screen reveals poly (ADP ribose)-regulated recruitment of the repressive polycomb and NuRD complexes to sites of DNA damage. *Proc. Natl Acad. Sci. USA*, **107**, 18475–18480.
21. LeRoy,G., Loyola,A., Lane,W.S. and Reinberg,D. (2000) Purification and characterization of a human factor that assembles and remodels chromatin. *J. Biol. Chem.*, **275**, 14787–14790.
22. Hanai,K., Furuhashi,H., Yamamoto,T., Akasaka,K. and Hirose,S. (2008) RSF governs silent chromatin formation via histone H2Av replacement. *PLoS Genet.*, **4**, e1000011.
23. Sheu,J.J., Guan,B., Choi,J.H., Lin,A., Lee,C.H., Hsiao,Y.T., Wang,T.L., Tsai,F.J. and Shih Ie,M. (2010) Rsf-1, a chromatin remodeling protein, induces DNA damage and promotes genomic instability. *J. Biol. Chem.*, **285**, 38260–38269.
24. Poot,R.A., Bozhenok,L., van den Berg,D.L., Steffensen,S., Ferreira,F., Grimaldi,M., Gilbert,N., Ferreira,J. and Varga-Weisz,P.D. (2004) The Williams syndrome transcription factor interacts with PCNA to target chromatin remodelling by ISWI to replication foci. *Nat. Cell Biol.*, **6**, 1236–1244.
25. Xiao,A., Li,H., Shechter,D., Ahn,S.H., Fabrizio,L.A., Erdjument-Bromage,H., Ishibe-Murakami,S., Wang,B., Tempst,P., Hofmann,K. *et al*. (2009) WSTF regulates the H2A.X DNA damage response via a novel tyrosine kinase activity. *Nature*, **457**, 57–62.
26. Yoshimura,K., Kitagawa,H., Fujiki,R., Tanabe,M., Takezawa,S., Takada,I., Yamaoka,I., Yonezawa,M., Kondo,T., Furutani,Y. *et al*. (2009) Distinct function of 2 chromatin remodeling complexes that share a common subunit, Williams syndrome transcription factor (WSTF). *Proc. Natl Acad. Sci. USA*, **106**, 9280–9285.
27. Varga-Weisz,P.D., Wilm,M., Bonte,E., Dumas,K., Mann,M. and Becker,P.B. (1997) Chromatin-remodelling factor CHRAC contains the ATPases ISWI and topoisomerase II. *Nature*, **388**, 598–602.
28. Ito,T., Bulger,M., Pazin,M.J., Kobayashi,R. and Kadonaga,J.T. (1997) ACF, an ISWI-containing and ATP-utilizing chromatin assembly and remodeling factor. *Cell*, **90**, 145–155.
29. Poot,R.A., Dellaire,G., Hulsmann,B.B., Grimaldi,M.A., Corona,D.F., Becker,P.B., Bickmore,W.A. and Varga-Weisz,P.D. (2000) HuCHRAC, a human ISWI chromatin remodelling complex contains hACF1 and two novel histone-fold proteins. *EMBO J.*, **19**, 3377–3387.
30. Hartlepp,K.F., Fernandez-Tornero,C., Eberharter,A., Grune,T., Muller,C.W. and Becker,P.B. (2005) The histone fold subunits of Drosophila CHRAC facilitate nucleosome sliding through dynamic DNA interactions. *Mol. Cell. Biol.*, **25**, 9886–9896.
31. Kukimoto,I., Elderkin,S., Grimaldi,M., Oelgeschlager,T. and Varga-Weisz,P.D. (2004) The histone-fold protein complex CHRAC-15/17 enhances nucleosome sliding and assembly mediated by ACF. *Mol. Cell*, **13**, 265–277.
32. Längst,G. and Becker,P.B. (2001) Nucleosome mobilization and positioning by ISWI-containing chromatin remodeling factors. *J. Cell Science*, **114**, 2561–2568.
33. Eberharter,A., Ferrari,S., Langst,G., Straub,T., Imhof,A., Varga-Weisz,P., Wilm,M. and Becker,P.B. (2001) Acf1, the largest subunit of CHRAC, regulates ISWI-induced nucleosome remodelling. *EMBO J.*, **20**, 3781–3788.
34. Corona,D.F.V., Längst,G., Clapier,C.R., Bonte,E.J., Ferrari,S., Tamkun,J.W. and Becker,P.B. (1999) ISWI is an ATP-dependent nucleosome remodeling factor. *Mol. Cell*, **3**, 239–245.
35. Alexiadis,V., Varga-Weisz,P.D., Bonte,E., Becker,P.B. and Gruss,C. (1998) *In vitro* chromatin remodelling by chromatin accessibility complex (CHRAC) at the SV40 origin of DNA replication. *EMBO J.*, **17**, 3428–3438.
36. Ura,K., Araki,M., Saeki,H., Masutani,C., Ito,T., Iwai,S., Mizukoshi,T., Kaneda,Y. and Hanaoka,F. (2001) ATP-dependent chromatin remodeling facilitates nucleotide excision repair of UV-induced DNA lesions in synthetic dinucleosomes. *EMBO J.*, **20**, 2004–2014.
37. Nightingale,K.P., Baumann,M., Eberharter,A., Mamais,A., Becker,P.B. and Boyes,J. (2007) Acetylation increases access of remodelling complexes to their nucleosome targets to enhance initiation of V(D)J recombination. *Nucleic Acids Res.*, **35**, 6311–6321.
38. Maier,V.K., Chioda,M., Rhodes,D. and Becker,P.B. (2008) ACF catalyses chromatosome movements in chromatin fibres. *EMBO J.*, **27**, 817–826.
39. Chioda,M., Vengadasalam,S., Kremmer,E., Eberharter,A. and Becker,P.B. (2010) Developmental role for ACF1-containing nucleosome remodellers in chromatin organisation. *Development*, **137**, 3513–3522.
40. Fyodorov,D.V., Blower,M.D., Karpen,G.H. and Kadonaga,J.T. (2004) Acf1 confers unique activities to ACF/CHRAC and promotes the formation rather than disruption of chromatin *in vivo*. *Genes Dev.*, **18**, 170–183.
41. Collins,N., Poot,R.A., Kukimoto,I., Garcia-Jimenez,C., Dellaire,G. and Varga-Weisz,P.D. (2002) An ACF1-ISWI chromatin-remodeling complex is required for DNA replication through heterochromatin. *Nat. Genet.*, **32**, 627–632.
42. Lan,L., Ui,A., Nakajima,S., Hatakeyama,K., Hoshi,M., Watanabe,R., Janicki,S.M., Ogiwara,H., Kohno,T., Kanno,S. *et al*. (2010) The ACF1 complex is required for DNA double-strand break repair in human cells. *Mol. Cell*, **40**, 976–987.
43. Franken,N.A., Rodermond,H.M., Stap,J., Haveman,J. and van Bree,C. (2006) Clonogenic assay of cells *in vitro*. *Nat. Protoc.*, **1**, 2315–2319.
44. Elbashir,S.M., Harborth,J., Lendeckel,W., Yalcin,A., Weber,K. and Tuschl,T. (2001) Duplexes of 21-nucleotide RNAs mediate RNA interference in cultured mammalian cells. *Nature*, **411**, 494–498.
45. Bozhenok,L., Wade,P.A. and Varga-Weisz,P. (2002) WSTF-ISWI chromatin remodeling complex targets heterochromatic replication foci. *EMBO J.*, **21**, 2231–2241.
46. Stopka,T. and Skoultchi,A.I. (2003) The ISWI ATPase Snf2h is required for early mouse development. *Proc. Natl Acad. Sci. USA*, **100**, 14097–14102.
47. Laird,C.D., Hansen,R.S., Canfield,T.K., Lamb,M.M. and Gartler,S.M. (1993) Chromosomal fragile sites: molecular test of the delayed-replication model. *Cold Spring Harb. Symp. Quant. Biol.*, **58**, 633–635.
48. Wang,L., Darling,J., Zhang,J.S., Huang,H., Liu,W. and Smith,D.I. (1999) Allele-specific late replication and fragility of the most active common fragile site, FRA3B. *Hum. Mol. Genet.*, **8**, 431–437.
49. Casper,A.M., Nghiem,P., Arlt,M.F. and Glover,T.W. (2002) ATR regulates fragile site stability. *Cell*, **111**, 779–789.
50. Arlt,M.F., Casper,A.M. and Glover,T.W. (2003) Common fragile sites. *Cytogenet. Genome Res.*, **100**, 92–100.
51. Glover,T.W., Arlt,M.F., Casper,A.M. and Durkin,S.G. (2005) Mechanisms of common fragile site instability. *Hum. Mol. Genet.*, **14 (Spec No. 2)**, R197–R205.
52. Xu,B., Kim,S.T., Lim,D.S. and Kastan,M.B. (2002) Two molecularly distinct G(2)/M checkpoints are induced by ionizing irradiation. *Mol. Cell. Biol.*, **22**, 1049–1059.
53. Park,J.H., Park,E.J., Lee,H.S., Kim,S.J., Hur,S.K., Imbalzano,A.N. and Kwon,J. (2006) Mammalian SWI/SNF

complexes facilitate DNA double-strand break repair by promoting gamma-H2AX induction. *EMBO J.*, **25**, 3986–3997.
54. Mortusewicz,O. and Leonhardt,H. (2007) XRCC1 and PCNA are loading platforms with distinct kinetic properties and different capacities to respond to multiple DNA lesions. *BMC Mol. Biol.*, **8**, 81.
55. Fyodorov,D.V. and Kadonaga,J.T. (2002) Binding of Acf1 to DNA involves a WAC motif and is important for ACF-mediated chromatin assembly. *Mol. Cell. Biol.*, **22**, 6344–6353.
56. Erdel,F., Schubert,T., Marth,C., Langst,G. and Rippe,K. (2010) Human ISWI chromatin-remodeling complexes sample nucleosomes via transient binding reactions and become immobilized at active sites. *Proc. Natl Acad. Sci. USA*, **107**, 19873–19878.
57. Matsuoka,S., Huang,M. and Elledge,S.J. (1998) Linkage of ATM to cell cycle regulation by the Chk2 protein kinase. *Science*, **282**, 1893–1897.
58. Celeste,A., Fernandez-Capetillo,O., Kruhlak,M.J., Pilch,D.R., Staudt,D.W., Lee,A., Bonner,R.F., Bonner,W.M. and Nussenzweig,A. (2003) Histone H2AX phosphorylation is dispensable for the initial recognition of DNA breaks. *Nat. Cell. Biol.*, **5**, 675–679.
59. Fernandez-Capetillo,O., Chen,H.T., Celeste,A., Ward,I., Romanienko,P.J., Morales,J.C., Naka,K., Xia,Z., Camerini-Otero,R.D., Motoyama,N. *et al.* (2002) DNA damage-induced G2-M checkpoint activation by histone H2AX and 53BP1. *Nat. Cell. Biol.*, **4**, 993–997.
60. Terzoudi,G.I., Manola,K.N., Pantelias,G.E. and Iliakis,G. (2005) Checkpoint abrogation in G2 compromises repair of chromosomal breaks in ataxia telangiectasia cells. *Cancer Res.*, **65**, 11292–11296.
61. Lobrich,M. and Jeggo,P.A. (2007) The impact of a negligent G2/M checkpoint on genomic instability and cancer induction. *Nat. Rev. Cancer*, **7**, 861–869.
62. Wang,X., Li,G.C., Iliakis,G. and Wang,Y. (2002) Ku affects the CHK1-dependent G(2) checkpoint after ionizing radiation. *Cancer Res.*, **62**, 6031–6034.
63. Lee,S.E., Moore,J.K., Holmes,A., Umezu,K., Kolodner,R.D. and Haber,J.E. (1998) Saccharomyces Ku70, mre11/rad50 and RPA proteins regulate adaptation to G2/M arrest after DNA damage. *Cell*, **94**, 399–409.
64. Shim,E.Y., Ma,J.L., Oum,J.H., Yanez,Y. and Lee,S.E. (2005) The yeast chromatin remodeler RSC complex facilitates end joining repair of DNA double-strand breaks. *Mol. Cell. Biol.*, **25**, 3934–3944.
65. Morrison,A.J., Highland,J., Krogan,N.J., Arbel-Eden,A., Greenblatt,J.F., Haber,J.E. and Shen,X. (2004) INO80 and gamma-H2AX interaction links ATP-dependent chromatin remodeling to DNA damage repair. *Cell*, **119**, 767–775.
66. van Attikum,H., Fritsch,O., Hohn,B. and Gasser,S.M. (2004) Recruitment of the INO80 complex by H2A phosphorylation links ATP-dependent chromatin remodeling with DNA double-strand break repair. *Cell*, **119**, 777–788.
67. Park,J.H., Park,E.J., Hur,S.K., Kim,S. and Kwon,J. (2009) Mammalian SWI/SNF chromatin remodeling complexes are required to prevent apoptosis after DNA damage. *DNA Repair*, **8**, 29–39.